Evaluation of the pharmacokinetic and pharmaceutical characteristics of exosomes for the development of exosome-based drug delivery carrier.

(エキソソームを利用したデリバリーキャリアの開発を目的とした体内動態および製剤学的特性の評価)

--Digest--

２０１８

CHAROENVIRIYAKUL CHONLADA

Contents

Preface

Intercellular communication is essential in multicellular organisms. Cells exchange information through various pathways. Cells communicate with neighbor cells by direct contact between cells such as gap junction. On the other hand, cells secrete molecules like hormones or cytokines that sends signal to distant cells. Besides these molecules, cells also secretes extracellular vesicles that transfer cargoes to their recipient cells[1]. Extracellular vesicles are roughly classified into three types based on their origin: apoptotic bodies, microvesicles, and exosomes [2]. Among these extracellular vesicles, exosomes have gained much attraction.

Exosomes are small membrane vesicles with a diameter of 30–120 nm that are secreted from various types of cells [3,4]. Since the discovery that exosomes act as intercellular communication tools by transferring their cargoes including proteins and nucleic acids to the recipient cells, the roles of exosomes in physiological events such as tumor metastasis and immune response have been vigorously investigated [5–7]. In addition, the possibility of the development of exosome-based drug delivery systems (DDS) has been demonstrated by several studies in which exosomes were used to deliver proteins and nucleic acids to specific types of target cells [8,9]. To exploit exosomes as drug delivery carriers, it is important to understand the factors affecting the pharmacokinetics of exosome, such as types of exosome-producing cells, and the role of surface protein on their pharmacokinetics. In addition, preservation method is an important issue to be concerned for the development of exosome-based drug delivery carriers. However, the information about these factors is limited.

Therefore, in this thesis, I investigated the pharmacokinetics of exosome from five different types of murine cell lines, and elucidated the role of exosome surface protein on their pharmacokinetics by developing method to label inner space of exosomes. In addition, I also developed a preservation method of exosomes utilizing lyophilization.

Chapter 1

Evaluation of cell type-specific and common characteristics of exosomes derived from mouse cell lines

1-1. Introduction

Exosomes are small membrane vesicles secreted from various types of cells, which transfer their cargoes, proteins and nucleic acids, to the recipient cells. Several studies demonstrate that exosomes can be exploited as drug delivery vehicles, which can deliver proteins and nucleic acids to specific types of target cells.

The yield of exosomes and the physicochemical properties that affect their pharmacokinetics, such as particle size and surface charge, may vary with the type of exosome-producing cell. Because these factors are expected to greatly influence the therapeutic efficacy of exosomes, it is necessary to select appropriate types of exosome-producing cells for the development of exosome-based DDS. Moreover, the exosome yield is an important factor for the development of exosome-based DDS, and the yield may vary among different types of cells. However, little information is available about how the yield, physicochemical properties, and pharmacokinetics of exosomes depend on the cell type.

In this chapter, five different types of murine cell lines, which represent whole body of mouse, were selected as model exosome-producing cells: B16BL6 melanoma cells, C2C12 myoblast cells, NIH3T3 fibroblasts cells, MAEC aortic endothelial cells, and RAW264.7 macrophage-like cells. B16BL6 cell line was selected because my laboratory reported the pharmacokinetics of B16BL6-derived exosomes. I also selected other 4 types of normal, not tumor, cell lines, because these cells were easily transfected and produced gLuc-LA-modified exosomes. I collected exosomes from these types of cells and evaluated the exosome yield by measuring protein amount and particle number. I then investigated the particle size and zeta potential of these exosomes. To evaluate the pharmacokinetics of exosomes after an intravenous injection into mice, a fusion protein of *Gaussia* luciferase (gLuc) and lactadherin (LA), gLuc-LA, was used to label the exosomes with gLuc [10]. The time course of the serum exosome concentration was examined by measuring the gLuc activity after an intravenous injection of gLuc-LA-labeled exosomes, and the biodistribution of the labeled exosomes was visualized using *in vivo* imaging.

1-2. Material and Methods

1-2-1. Cell culture

B16BL6 cells were obtained from the Cancer Chemotherapy Center of the Japanese Foundation for Cancer Research. C2C12, NIH3T3, and RAW264.7 cells were purchased from the American Type Culture Collection. MAEC cells were a gift from Professor Ichiro Saito (Department of Pathology, Tsurumi University School of Dental Medicine, Yokohama, Japan). B16BL6 cells, C2C12 cells, and NIH3T3 cells were cultured in Dulbecco's modified Eagle's minimum essential medium (Nissui Pharmaceutical, Tokyo, Japan) supplemented with 10% fetal bovine serum (FBS) and penicillin/streptomycin/L-glutamine (PSG). RAW264.7 cells were cultured in Roswell Park Memorial Institute medium (Nissui Pharmaceutical, Tokyo, Japan) supplemented with 10% FBS and PSG. MAEC cells were cultured in medium 199 (Gibco, Grand Island, NY, USA) supplement with 10% FBS and PSG. Cells were cultured at 37°C in humidified air containing 5% CO_2.

1-2-2. Collection of exosomes

Culture media used for exosome collection were prepared by ultracentrifugation at 100,000 × g for 2 h to remove FBS-derived exosomes. To reach approximately 80% confluency after 24 h incubation, cells were seeded into 15-cm dishes at the following numbers: 8×10^6 cells for B16BL6 and C2C12, 7×10^6 cells for NIH3T3, 5×10^6 cells for MAEC, and 2×10^7 cells for RAW264.7. Twenty-four hours after cell seeding, the medium was replaced with exosome-depleted medium and incubation was resumed for another 24 h. At the time of harvesting exosomes, the confluency of cells was almost 100% for all the cases examined. Exosomes in the supernatant were purified using a previously described procedure [10]. In brief, cell debris and large vesicles were cleared from the supernatant by sequential centrifugation and filtration using a 0.2 μm filter. Subsequently, the supernatant was subjected to ultracentrifugation at 100,000 × g for 1 h to sediment the exosomes. The exosomes were washed twice with phosphate-buffered saline (PBS). The amount of collected exosomes was estimated by measuring the protein concentration

using the Quick Start Bradford protein assay (BioRad, Hercules, CA, USA), according to the manufacturer's instructions, and by measuring the particle number using a qNano instrument (Izon Science Ltd., Christchruch, New Zealand). Exosomes labeled with gLuc-LA were collected as previously described [11]. In brief, exosome-producing cells were transfected with gLuc-LA-expressing plasmid vectors using polyethylenimine "Max" (Polysciences, Warrington, PA, USA) and were incubated for 24 h. Exosomes in the culture supernatant were collected as described above. Exosomes labeled with gLuc-LA were mixed with a sea pansy luciferase assay system (Picagene Dual; Toyo Ink, Tokyo, Japan), and their chemiluminescence was measured with a luminometer (Lumat LB 9507; EG&G Bethhold, Bad Wildbad, Germany) to estimate gLuc activity. For immunofluorescent experiment, exosomes were labelled with PKH26 dye (Sigma-Aldrich) as previously described [10]. All the collected exosomes were aliquoted to avoid multiple freeze-thaw cycles and were stored at -80ºC until use. Storage of exosomes at -80ºC had negligible effect on their physicochemical properties.

1-2-3. Western blotting

Cell lysates were prepared using a freeze–thaw procedure followed by centrifugation to remove the cell debris. Western blotting was performed as previously described [11,12]. In brief, reduced exosomes and cell lysate samples (1.5 μg protein for Alix, HSP70, and calnexin and 5 μg protein for CD81) were loaded onto a 10% sodium dodecyl sulphate-polyacrylamide gel, were subjected to electrophoresis, and were then transferred to a polyvinylidene fluoride transfer membrane. The membrane was incubated with Alix-specific antibody (1:20,000 dilution; BD Biosciences, San Jose, CA, USA), HSP70-specific antibody (1:1000 dilution; Cell Signaling Technology, Danvers, MA, USA), CD81-specific antibody (1:200 dilution; Santa Cruz Biotechnology, CA, USA), or calnexin-specific antibody (1:1000 dilution; Santa Cruz) overnight at 4°C. The membranes were then incubated with horseradish peroxidase (HRP)-conjugated rabbit anti-mouse IgG antibody (1:2000 dilution; Thermo Fisher, Waltham, MA, USA) or goat anti-rabbit IgG antibody (1:5000 dilution; Santa Cruz Biotechnology) for 1 h at room temperature.

The membrane was reacted with Immobilon Western Chemiluminescent HRP Substrate (Merck Millipore, Billerica, MA, USA), and chemiluminescence was detected using an LAS-3000 instrument (FUJIFILM, Tokyo, Japan).

1-2-4. Transmission electron microscopy

Exosomes were mixed with an equal volume of 4% paraformaldehyde in PBS. The mixture was applied to a carbon Formvar film-coated transmission electron microscopy (TEM) grid (Alliance Biosystems, Osaka, Japan) and was incubated for 20 min at room temperature. After washing with PBS, the samples were fixed with 1% glutaraldehyde for 5 min. After washing with distilled water, the grid was stained with 1% uranyl acetate for 2 min, and the samples were observed using TEM (Hitachi H-7650; Hitachi High-Technologies Corporation, Tokyo, Japan)

1-2-5. Particle size distribution and zeta potential of exosomes

A qNano instrument was used to measure the particle size distribution of the exosomes. A Zetasizer Nano ZS (Malvern Instruments, Malvern, UK) was used to determine the zeta potential of the exosomes.

1-2-6. Animals

Five-week-old male BALB/c mice were purchased from Japan SLC, Inc. (Shizuoka, Japan). All protocols for the animal experiments were approved by the Animal Experimentation Committee of the Graduate School of Pharmaceutical Science of Kyoto University.

1-2-7. Pharmacokinetic studies

Exosomes labeled with gLuc-LA were intravenously injected into mice via the tail vein at a dose of 5 μg/200 μl/shot. Blood samples were collected at the indicated time points. Serum was obtained by centrifuging clotted whole blood at 8000 × g for 20 min at 4°C. These serum samples were diluted with PBS, and their chemiluminescence was then measured as described

above. The amount of exosomes in each sample was normalized to that of the injected dose based on the gLuc activity and was expressed as the percent of the injected dose/ml (% ID/ml). The area under the curve (AUC) and the mean residence time were calculated for each animal by integration to 4 h. The clearance (CL) was calculated by dividing the injected dose by the AUC. The half-life ($t_{1/2\alpha}$) was calculated as previously described [11].

1-2-8. Chemiluminescence imaging of exosomes *in vivo*

Mice received intravenous injections of gLuc-LA-labeled exosomes at a dose of 5 μg/200 μl/shot. Five minutes after the administration, chemiluminescent images were acquired using an IVIS Spectrum *in vivo* imaging system (Caliper Life Science, Hopkinton, MA, USA). Immediately before imaging, 100 μg of coelenterazine (Regis Technologies, Morton Grove, IL, USA), a substrate for gLuc, was injected into the tail vein of each mouse.

1-2-9. Immunofluorescent staining of macrophages

Exosomes labelled with PKH26 dye were injected into mice via the tail vein at a dose of 5 μg/200 μl/shot. Five minutes after injection, mice were sacrificed, and the liver was harvested. The harvested organs were frozen at -80ºC, and the frozen sections were prepared by using a freezing microtome (Leica CM3050 S; Leica Biosystems, Germany). The sections were stained with Alexa Fluor488-labelled anti-mouse F4/80 antibody (Biolegend, San Diego, CA, USA) as previously described [11].

1-3. Results

1-3-1. Exosomes were collected from five different cell types

Exosomes collected from five different cell types were positive for the exosome marker proteins Alix, HSP70, and CD81, although there were differences in the amounts of these marker proteins among the exosomes (Fig. 1a). In particular, exosomal expression of CD81 was highly variable among the different cell types. Exosome samples were negative for calnexin, an

endoplasmic reticulum marker, suggesting that the collected exosome samples were not contaminated with cell debris. Figure 1b shows the TEM images of the exosomes. Globular vesicles of approximately 100 nm in diameter were observed in all the exosome samples.

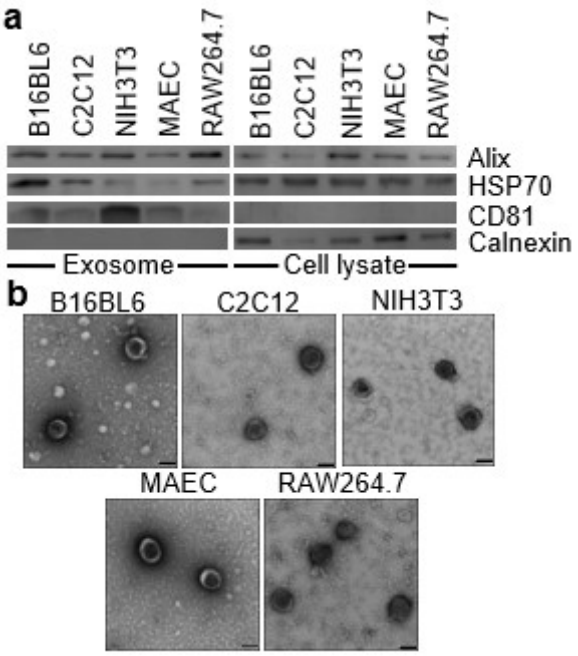

Figure 1. Collection of exosomes from five different cell types. (a) Western blotting analysis of the Alix, HSP70, CD81, and calnexin present in the exosomes and cell lysates derived from B16BL6, C2C12, NIH3T3, MAEC, and RAW264.7 cells. (b) Transmission electron microscopy images of exosomes derived from B16BL6, C2C12, NIH3T3, MAEC, and RAW264.7 cells. Scale bar = 100 nm.

1-3-2. Yield of exosomes was dependent on cell type

Figure 2 shows the amount of protein and the number of exosome particles collected from the supernatant of each culture dish after an incubation

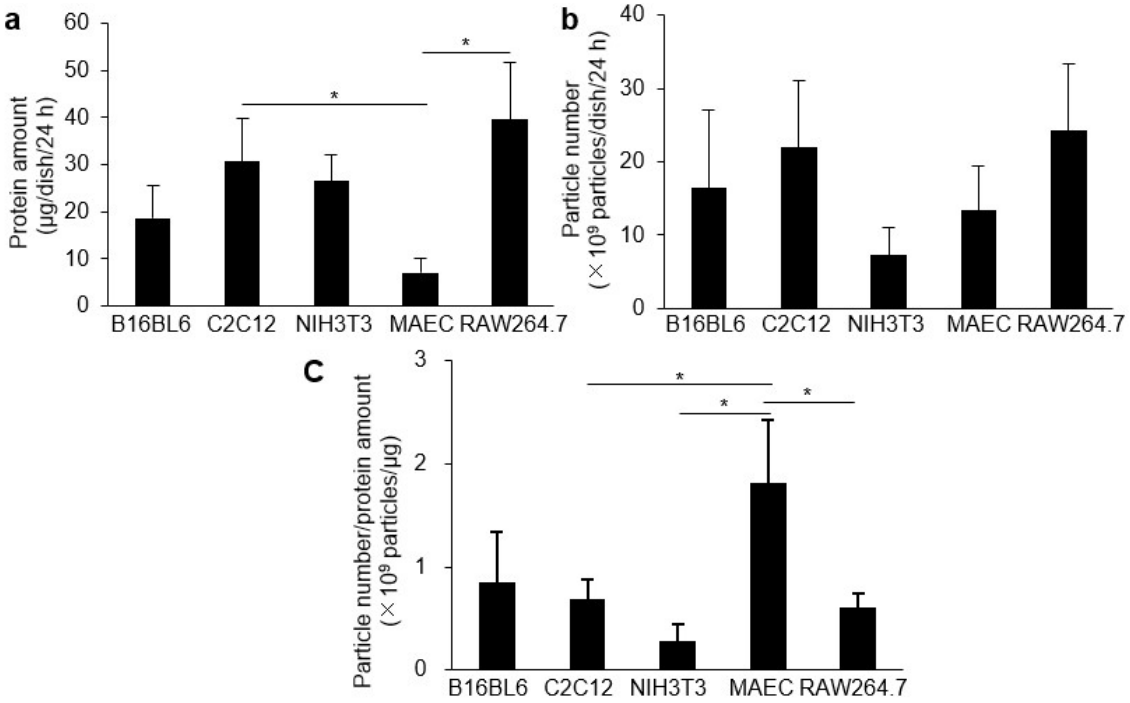

Figure 2. Amount of exosomes secreted from different cell types. Exosomes were collected from the supernatant of cells cultured for 24 h. (a) Amount of protein present in exosomes estimated using the Bradford assay. (b) Numbers of exosome particle estimated using a qNano instrument. (c) The ratio of exosome particles per μg protein. These results are expressed as the mean ± standard deviation (n = 3). *p < 0.05.

period of 24 h. Both parameters showed that C2C12 and RAW264.7 cells produced more exosomes than the other cell types. As for the particle number/protein amount ratio, MAEC showed the highest ratio, whereas NIH3T3 showed the lowest ratio among the cell types investigated in this study.

1-3-3. Exosomes were approximately 100 nm in diameter and possessed a negative charge

Figure 3 shows histograms of the particle size distributions of the exosomes. All the exosomes showed similar particle size distributions. Table 1 summarizes the median particle sizes and mean zeta potentials of the exosomes. All the exosomes were approximately 100 nm in diameter and possessed a negative zeta potential of approximately −40 mV.

Table 1. Particle sizes and zeta potentials of the exosomes from different cell types

Exosome-producing cells	Size (nm)	Zeta potential (mV)
B16BL6	100 ± 4	−39.2 ± 0.9
C2C12	111 ± 10	−38.9 ± 1.1
NIH3T3	106 ± 2	−35.3 ± 0.5
MAEC	102 ± 7	−41.6 ± 1.5
RAW264.7	105 ± 4	−38.8 ± 0.6

Results are expressed as the mean ± standard deviation (n = 3).

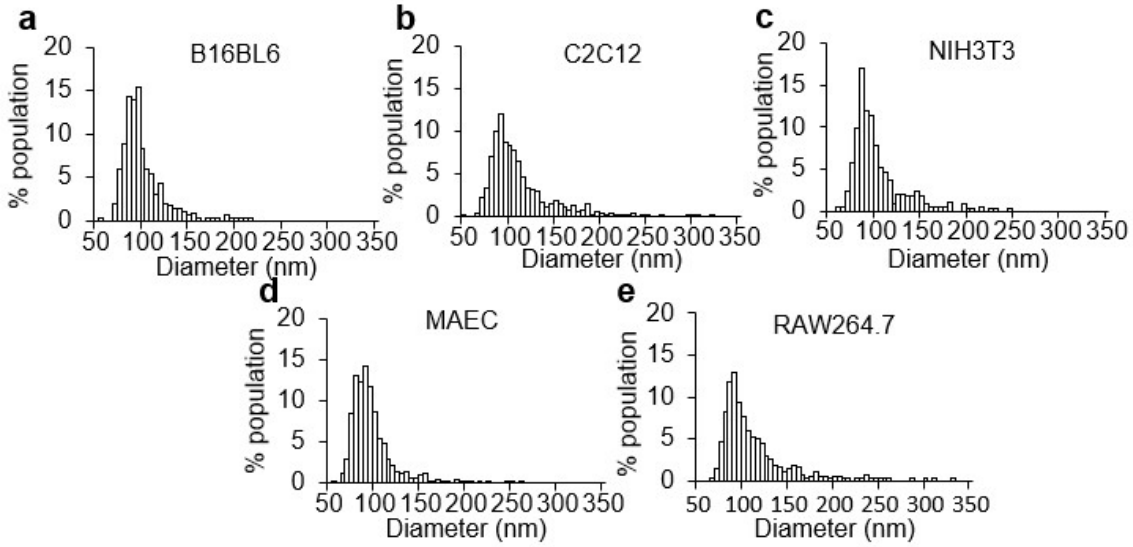

Figure 3. Exosome particle size distribution. Representative histograms of the exosome particle size distributions obtained from (a) B16BL6, (b) C2C12, (c) NIH3T3, (d) MAEC, and (e) RAW264.7 cells, determined using a qNano.

1-3-4. Exosomes were rapidly eliminated from the circulation and mainly distributed to the liver

To evaluate the pharmacokinetics of the exosomes, gLuc-LA-labeled exosomes were intravenously injected into mice. The structural and physicochemical properties of the gLuc-LA-labeled exosomes were compared with those of the unlabeled ones (data not shown). After intravenous injections into mice, serum gLuc activity immediately decreased regardless of the source of exosomes, indicating that all the exosomes were rapidly eliminated from the circulation (Fig. 4). Table 2 shows the pharmacokinetic parameters of the exosomes calculated from their serum concentration profiles. These parameters were not remarkably different among all the exosomes.

To investigate the biodistribution of the exosomes, gLuc-LA-labeled exosomes were visualized 5 min after intravenous injection using *in vivo* imaging. All the exosomes mainly distributed to the liver (Fig. 5). These results indicate that all the exosomes investigated in this study have similar biodistribution properties.

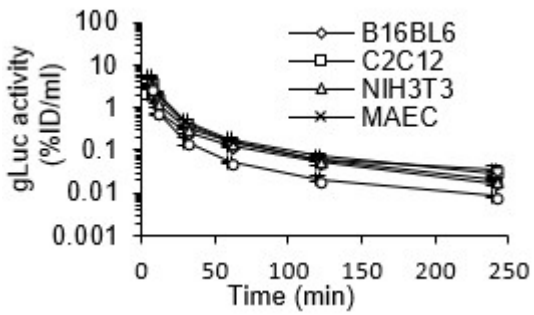

Figure 4. Time-course of serum gLuc activity after intravenous injection of gLuc-LA-labeled exosomes. Serum gLuc activity was measured after intravenously injecting gLuc-LAlabeled exosomes collected from B16BL6 (rhombus), C2C12 (square), NIH3T3 (triangle), MAEC (cross), or RAW264.7 (circle) cells. These results are expressed as the mean ± standard deviation (n = 4).

Table 2. Pharmacokinetic parameters of gLuc-LA labeled exosomes after intravenous injection

Exosome-producing cells	$t_{1/2\alpha}$ (min)	AUC (% of dose·h/ml)	MRT (h)	CL (ml/h)
B16BL6	3.81 ± 0.68	0.897 ± 0.150	0.511 ± 0.069	114 ± 19
C2C12	4.08 ± 0.52	1.54 ± 0.35	0.435 ± 0.049	67.1 ± 13.3
NIH3T3	3.92 ± 1.04	1.27 ± 0.10	0.428 ± 0.034	78.9 ± 5.9
MAEC	3.95 ± 0.73	1.87 ± 0.17	0.383 ± 0.022	53.7 ± 4.6
RAW264.7	2.77 ± 0.28	0.945 ± 0.075	0.261 ± 0.024	106 ± 8.6

These results are expressed as the mean ± standard deviation (n = 4).

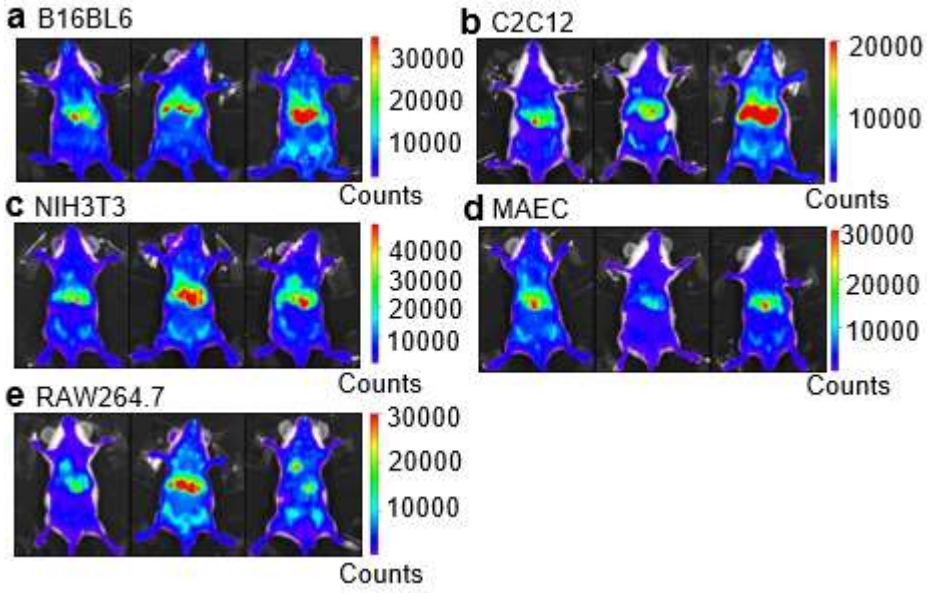

Figure 5. *In vivo* imaging of gLuc-LA-labeled exosomes. The biodistribution of gLuc-LA-labeled exosomes inmicewas imaged using a bolus intravenous injection of coelenterazine 5min after the intravenous injection of exosomes obtained from (a) B16BL6, (b) C2C12, (c) NIH3T3, (d) MAEC, or (e) RAW264.7 cells.

1-3-5. Exosomes labelled with PKH26 were taken up by macrophages

To evaluate the type of liver cells that take up exosomes, PKH26-labelled exosomes were injected into mice via tail vein. Most of the red signal derived from PKH26-labelled exosomes was co-localized with F4/80+ cells stained with Alexa Fluor488 (green)-labelled antibody in the liver (Fig. 6), indicating that all types of exosomes used in this study were taken up by macrophages in the liver. In addition, previous data of my laboratory [11] showed that the clearance of B16BL6-derived exosomes was drastically delayed in macrophage-depleted mice. To investigate the role of macrophages on the clearance of other types of exosomes, all types of exosomes except B16BL6-exosomes were injected into macrophage-depleted mice. Clearance of all types of exosomes in macrophage-depleted mice

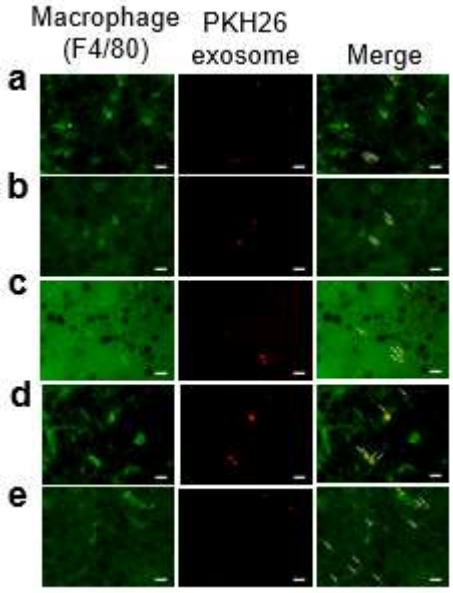

Figure 6. Macrophage uptake of exosomes labeled with PKH26. Cryostat sections of liver collected from mice receiving PKH26 (red)-labeled exosomes derived from (a) B16BL6, (b) C2C12, (c) NIH3T3, (d) MAEC, or (e) RAW264.7 cells. Macrophages were stained with F4/80-specific antibody (green). Scale bar = 10 μm.

was significantly delayed compared to that in untreated mice (Fig. 7), indicating that macrophages play a key role in the clearance of exosomes from blood circulation irrespective of the cell type.

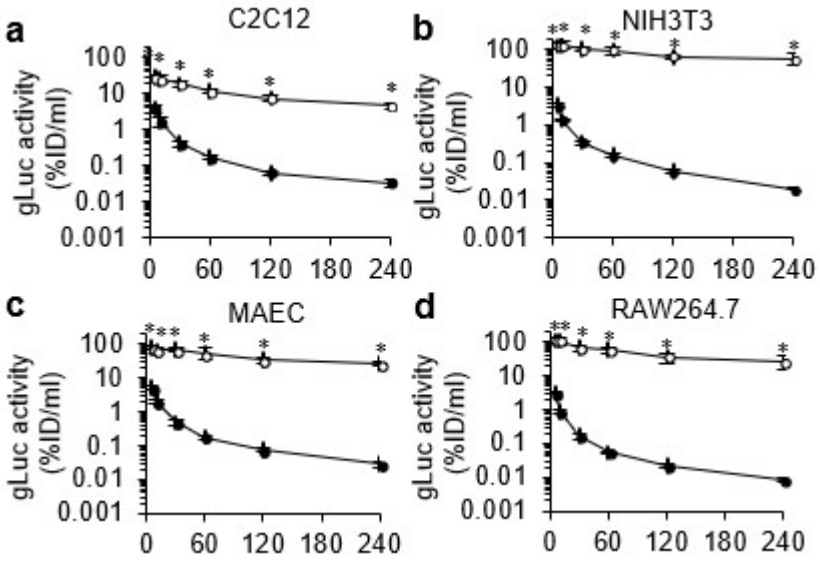

Figure 7. Clearance of exosome was delayed in macrophage-depleted mice. gLuc activity in the serum of untreated mice (closed symbols) and macrophage-depleted mice (opened symbol) was sequentially measured after intravenous injection of gLuc-LA-labelled exosomes derived from (a) C2C12, (b) NIH3T3, (c) MAEC, or (d) RAW264.7 cells. These results are expressed as the mean ± standard deviation (n = 4).

1-4. Discussion

Each cell type produced a different amount of exosomes. Among the cells investigated in the present study, RAW264.7 and C2C12 produced the largest amounts of exosomes. In addition, MAEC cells showed the highest particle number/protein amount ratio, whereas NIH3T3 cells showed the lowest particle number/protein amount ratio among the cell types investigated in the present study (Fig. 1a). This suggests that protein level on the exosome membrane or in the cargo is different depending on the cell type. A previous study showed that myotubes produced approximately 20 times as many exosomes as myoblasts did [13]. In previous studies on the application of exosomes as a delivery vehicle, the dose of exosomes in mice varied from 1 to 150 μg [8,14,15] and the dose of exosomes in rats varied from 50 to 250 μg [16,17]. The exosome yield of the cells investigated in this study might be enough for a dose of 1–10 μg but not for a dose of ≥150 μg because at least four 15-cm dishes are required for a single dose of 150 μg. It has been reported

that culturing cells under low pH conditions increased the yield of exosomes [18] and that an increase in cytosolic Ca^{2+} concentration stimulated exosome secretion from cells [19]. Exploitation of these methods to increase the yield of exosomes would be necessary if the exosome-based DDS required a high dose of exosomes.

Analysis of the physicochemical properties of the exosomes demonstrated that all the investigated exosomes were approximately 100 nm in diameter and had a negative zeta potential, which are consistent with preceding studies investigating the exosomes produced by the same or different cell types [20–23]. The particle size of the exosomes, a factor that will affect their pharmacokinetics, was comparable among the exosomes collected from the different cell types. In contrast, the expression levels of CD81, a tetraspanin, in the exosomes were different among the different cell types (Fig. 1a). Previous studies used fluorescein intensity measurements to demonstrate that tetraspanins, such as Tspan8, play important roles in the target cell specificity and tissue distribution of fluorescein-labeled exosomes in rats [17,24]. In addition, an *in vitro* study demonstrated that CD81 is important for the CD29-dependent cellular uptake of exosomes derived from mesenchymal stem cells (MSC) in MSC themselves [25]. However, the present study revealed that the pharmacokinetics at the whole body level were similar for the exosomes derived from the five cell types investigated here. This indicates that differences in CD81 level have no significant influence on the pharmacokinetics of the exosomes in terms of serum concentration profile or biodistribution analyzed by *in-vivo* imaging.

I demonstrated that all the exosomes investigated in this study quickly disappeared from the systemic circulation and mainly distributed to the liver after intravenous injection (Fig. 4 and 5). This finding is consistent with the previous studies that investigated the pharmacokinetics of exosomes collected from various cell types [12,26,27]. In addition, the finding that exosomes distributed to the liver were mainly taken up by $F4/80^{+}$ macrophages irrespective of the type of exosome-producing cells is also in good agreement with the result of previous study of my laboratory obtained by using B16BL6-derived exosomes [11]. Moreover, this and previous study showed that the rapid clearance of exosomes from the systemic circulation was drastically delayed

in macrophage-depleted mice prepared using clodronate-containing liposome, which indicates that macrophages play a major role in the CL of exosomes, irrespective of the type of cell producing the exosomes. It is known that macrophages efficiently take up apoptotic cells through the recognition of phosphatidylserine (PS) on their surfaces [28]. Exosomes also expose PS on their outer leaflet [29]. In addition, it has been recently reported that scavenger receptor class A family on the surface of macrophages in the liver played an important role in the uptake of extracellular vesicles [30], which is also in agreement with the findings of the current study.

In Chapter 1, I demonstrated that different cell types produced different yields of exosomes. Exosomes had comparable physicochemical and pharmacokinetics properties irrespective of types of exosome-producing cells. These findings may provide information for development of exosome-based DDS from the viewpoint of productivity of exosomes.

Chapter 2

Evaluation of the role of exosome surface proteins in the pharmacokinetics of exosome

2-1. Introduction

In the development of exosome-based drug delivery carriers, pharmacokinetics of exosomes at the whole-body level is an important issue. My laboratory previously showed that Kupffer cells in the mouse liver take up intravenously administered exosomes through the recognition of phosphatidylserine (PS) on exosomes [31]. In addition to phospholipids, it is critical to elucidate the roles of surface proteins of exosomes in the pharmacokinetics of exosome. There is little information about the role of exosome surface proteins in the pharmacokinetics of exosomes at the whole-body level, though the role of several proteins on the surface of exosomes such as tetraspanins and integrins, on the *in vivo* behavior of exosomes have been investigated. For example, it has been shown that tetraspanin Tspan8 contributes to target cell selection of exosomes [17]. Moreover, the involvement of integrins $\alpha_6\beta_4$ and $\alpha_v\beta_5$ on exosomes in cellular uptake as well as in tumor metastasis was demonstrated [32].

In Chapter 1, I tracked the whole-body distribution of exosomes by using a fusion protein termed gLuc-LA. Evaluation of the pharmacokinetics of exosome treated with proteinases would be a direct approach to estimate the contribution of surface proteins of exosomes to the pharmacokinetics of exosomes. However, gLuc-LA cannot be used for this purpose because gLuc-LA on the outer surface of exosomes would be digested by the proteinase treatment.

In this chapter, I developed a novel method to label the inner space of exosomes by using Gag protein, which is derived from Moloney murine leukemia virus (MLV). Gag localizes to the inside of plasma membrane [33] through an interaction between the polybasic region of the Gag protein and phosphatidylinositol 4,5-bisphosphate in the plasma membrane [34]. I labeled exosomes derived from B16BL6 melanoma cells through transfection of a plasmid encoding a fusion protein consisting of the Gag protein and gLuc, which I termed Gag-gLuc. Then, to confirm that Gag-gLuc exosomes could be used to examine the role of exosome surface proteins on pharmacokinetics at the whole-body level in mice, I evaluated the expression level, stability and proteinase resistance of the Gag-gLuc-labeled exosomes. Next, I evaluated the physicochemical properties of non-treated and proteinase K (ProK)-treated exosomes. Furthermore, as Gag-gLuc

localizes to the inner space of exosome, Gag-gLuc-labeled exosomes can be treated with ProK without reducing gLuc activity. Therefore, I evaluated effect of surface proteins of exosomes on their pharmacokinetics by using the labeled exosome treated with ProK.

2-2. Material and Methods

2-2-1. Plasmid DNA (pDNA)

pDNA encoding gLuc-LA was obtained as described in Chapter 1. The coding sequence of Gag, the codon sequence of which was optimized to maximize protein expression in a murine host, was synthesized by Genscript (Piscataway, NJ, USA). gLuc coding sequence was obtained as described in a previous report [35]. Coding sequence of enhanced green fluorescent protein (GFP) was prepared from the pEGFP-N1 vector (BD Biosciences Clontech, Palo Alto, CA, USA). The coding sequence of murine CD63 was purchased from Open Biosystems (Thermo Fisher Scientific, Tokyo, Japan). The chimeric sequences of CD63-gLuc, GFP-LA, Gag-GFP, gLuc-LA and Gag-gLuc were prepared by using 2-step PCR method as described in a previous report [10]. The Gag polyprotein p65 of Moloney murine leukemia virus was used in Gag-based fusion proteins. All of the sequences encoding fusion proteins were subcloned into the BamHI/Xbal site of the pcDNA3.1 vector (Thermo Fisher Scientific) to construct pCMV vectors encoding corresponding fusion proteins.

2-2-2. Cell culture

Murine melanoma B16BL6 cells were cultured as described in Chapter 1. Mouse peritoneal macrophages were collected form 5-week-old male BALB/c mice and cultured using a previously described method [31].

2-2-3. Collection of exosomes

Exosomes were collected as describe in Chapter 1. For exosomes labeled with Gag-gLuc or gLuc-LA, Gag-gLuc exosomes and gLuc-LA exosomes were lysed by lysis buffer (Pierce;

Thermo Scientific, Illinois, USA), mixed with a sea pansy luciferase assay system (Picagene Dual; Toyo Ink, Tokyo, Japan), and their chemiluminescence was measured with a luminometer (Lumat LB 9507; EG&G Bethhold, Bad Wildbad, Germany) to estimate gLuc activity. For the preparation of ProK-digested exosome, 250 μg/ml of exosome was treated with 50 μg/ml of proteinase K (Nacalai Tesque, Inc. Kyoto, Japan) for 30 min at 37 ºC. After the digestion, ProK was inhibited by incubation with 5 mM phenylmethylsulfonyl fluoride (PMSF) for 10 min at 37 ºC. Then, the samples were washed by ultracentrifugation. For uptake and distribution experiment, exosome were labeled with PKH67 (Sigma-Aldrich, St. Louis, MO, USA) and PKH26 (Sigma-Aldrich) dye, respectively, as previously described [10]. All the collected exosome samples were aliquoted to avoid multiple freeze-thaw cycles and were stored at -80 ºC until use.

2-2-4. Transmission electron microscopy

TEM observation were perform as described in Chapter 1

2-2-5. Particle size distribution and zeta potential of exosomes

Particle size distribution and zeta potential of exosomes were obtained as described in Chapter 1

2-2-6. Stability of gLuc activity and binding of Gag-gLuc and gLuc-LA to exosome in serum

Stability of exosome labeling by Gag-gLuc and gLuc-LA in the serum were evaluated as previously described [11]. In brief, samples were incubated at 37 ºC in 20% FBS in PBS solution for 4 h. Stability of gLuc enzyme activity was evaluated by measuring gLuc activity of the collect samples. Release of Gag-gLuc of gLuc-LA from exosome was evaluated by ultracentrifugation of samples at 100,000 $\times g$ 1 h at 4 ºC to pellet the exosome. Then, the amount of Gag-gLuc or gLuc-LA bound to the exosome was evaluated by estimating Gag-gLuc or gLuc-LA released from the exosome as gLuc activity in the supernatant.

2-2-7. Sodium dodecyl sulphate-polyacrylamide gel electrophoresis (SDS-PAGE) of exosome samples followed by Coomassie Brilliant Blue (CBB) staining

Exosome samples were reduced with dithiothreitol (Nacalai Tesque, Inc. Kyoto, Japan) at 95 ºC for 3 min. The reduced samples were loaded onto a 10% sodium dodecyl sulphate-polyacrylamide gel and were subjected to electrophoresis. The gel was stained in CBB R-250 (Wako Pure Chemical, Osaka, Japan) for 30 min at room temperature, and destained by soaking in aqueous solution containing 7.5% acetic acid and 25% ethanol for 30 min twice. The stained gel was observed using an LAS-3000 instrument (FUJIFILM, Tokyo, Japan).

2-2-8. Western blotting

Western blotting was performed as described in Chapter 1. For antibody of integrin, integrin α_6-specfic antibody (1:1,000; Cell Signaling Technology, Danvers, MA, USA) or integrin β_1-specific antibody (1:1,000; Cell Signaling Technology) were used.

2-2-9. Resistance of exosome luciferase activity to ProK treatment

Exosome samples labeled with gLuc were incubated with ProK at final concentration of 50 μg/ml at 37 ºC for 30 min. Then, 5 mM PMSF was added to the samples at 37 ºC for 10 min to inhibit ProK activity. The samples were subsequently lysed with lysis buffer and gLuc activity was measured. The gLuc activity of samples digested with ProK were calculated as the percentage of gLuc activity of untreated samples.

2-2-10. Animals

Protocols for the animal experiments were as described in Chapter 1.

2-2-11. Pharmacokinetic studies

Experiment were performed as described in Chapter 1. About dose of injection, untreated and ProK-treated Gag-gLuc labeled exosomes were intravenously injected into mice

via the tail vein at a dose of 1.4 $\times 10^{10}$ RLU/200 μl/shot (corresponding to about 8 μg/shot for untreated exosomes).

2-2-12. Macrophage uptake of exosome

Peritoneal macrophages seeded in 96-well plate (2 $\times$ 10^5 cells/well) were incubated with untreated or ProK-treated exosome labeled with PKH67 with a dose of the same fluorescence intensity (corresponding to 2.8 and 14.0 μg/ml of untreated exosome for low and high doses, respectively). Cells were then incubated at 37 ºC for 2 h, washed twice with PBS, and harvested. Mean fluorescence intensity (MFI) of the cells was measured by a flow cytometer (Gallios Flow Cytometer; Beckman Coulter, Miami, FL) to estimate the amount of exosome taken up by the cells. The data were analyzed using Kaluza software (version 1.0, Beckman Coulter)

2-2-13. Immunofluorescent staining of macrophages

Untreated or ProK-treated exosomes labeled with PKH26 were intravenously administered to mice with the same level of fluorescence intensity (corresponding to 3.4 μg/shot for untreated exosome). Ten minutes after administration, mice were reperfused with PBS and the liver was harvested. The Sections of liver were harvested and stained as described in Chapter 1. Twenty fields/section were viewed at 10× magnification under fluorescence microscopy (biozero BZ-8000; Keyence, Osaka, Japan). The number of red fluorescence signals in each field was counted using BZ-X analyzer software (Keyence).

2-2-14. Lung distribution of intravenously-administered exosomes

Untreated or ProK-treated exosomes labeled with PKH26 were intravenously administered to mice with the same level of fluorescence intensity (corresponding to 3.4 μg/shot for untreated exosome). Ten minutes after administration, mice were sacrificed, reperfused with PBS and the lungs were harvested. The harvested lungs were frozen at −80 ºC and sections were

prepared using a freezing microtome (Leica CM3050 S, Leica Biosystems, Eisfeld, Germany). Twenty fields/section were viewed at 10× magnification under fluorescence microscopy (biozero BZ-8000). The number of red fluorescence signals in each field were counted using BZ-X analyzer software.

2-2-15. Statistical analysis

Differences among data sets were statistically analyzed by either the Student's t-test for paired comparison or one-way analysis of variance (ANOVA), followed by Fisher's Protected Least Significant Difference (PLSD) test for multiple comparisons.

2-3. Results

2-3-1 Exosomes collected from cells transfected with Gag-gLuc and gLuc-LA expressing plasmid showed luciferase activity

To evaluate the efficacy of gLuc labeling by the Gag-gLuc, gLuc-LA or CD63-gLuc fusion proteins, I measured the luciferase activity of cell lysates, culture media, supernatant obtained after ultracentrifugation and exosome samples collected from cells transfected with Gag-gLuc-, gLuc-LA or CD63-gLuc-expressing pDNA. As CD63 has been often used to modify exosome membranes [36–40], CD63-gLuc was used for comparison. While the gLuc activity of cell lysates and media of the Gag-gLuc group was comparable to that of CD63-gLuc group (0.57-fold compared to CD63-gLuc), gLuc activity of Gag-gLuc exosomes was 133-fold higher than that of CD63-gLuc exosomes. However, gLuc-LA exosomes showed 35-fold higher gLuc activity than Gag-gLuc exosomes (Fig. 8).

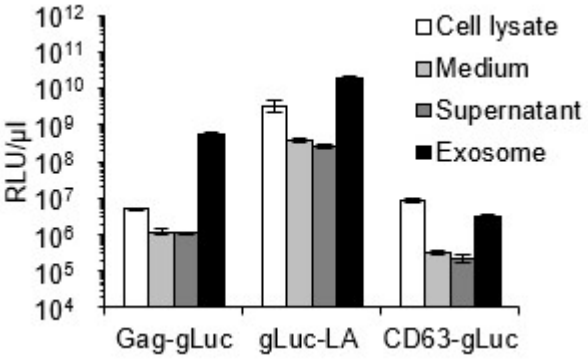

Figure 8. Exosomes can be labeled by Gag-gLuc. Luciferase activity of cell lysate (white), culture medium (light gray), supernatant after first ultracentrifugation (dark gray), and exosomes (black) collected from B16BL6 cells after transfection with Gag-gLuc, gLuc-LA, and CD63-gLuc. RLU: relative luminescence units.

2-3-2. gLuc labeling of Gag-gLuc exosome was stable in serum

gLuc activity of Gag-gLuc exosomes and gLuc-LA exosomes was stable after incubation in 20% FBS in PBS for four hours (Fig. 9a). I found that gLuc activity of Gag-gLuc exosome and gLuc-LA were 105.3% and 93.1%, respectively. Then, to evaluate the release of gLuc labeling from exosomes, Gag-gLuc EVs and gLuc-LA exosomes were incubated in 20% FBS in PBS for four hours and were subjected to ultracentrifugation to evaluate the release of gLuc from exosomes (Fig. 9b). I found that 94.4% and 96.0% of the gLuc activity of Gag-gLuc exosome and gLuc-LA exosome, respectively, were retained, which indicates that gLuc labeling of exosomes by Gag-gLuc and gLuc-LA was stable in the serum.

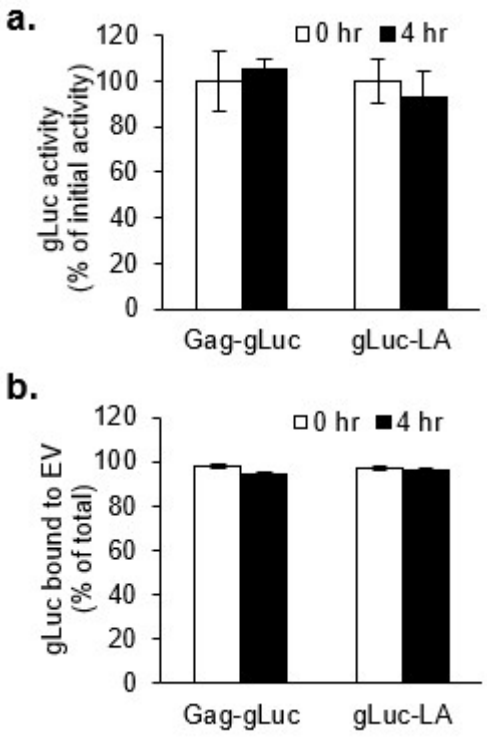

Figure 9. Exosomes labeled with Gag-gLuc and gLuc-LA were stable in serum for 4 h. Gag-gLuc exosomes and gLuc-LA exosomes were incubated in 20% FBS in PBS for 4 h. (a) Stability of gLuc activity was evaluated by measuring luciferase activity of collected samples. (b) Release of Gag-gLuc and gLuc-LA from exosomes was evaluated by measuring luciferase activity of ultracentrifugation supernatant. The data are expressed as the mean ± standard deviation (n = 3).

2-3-3. gLuc activity of Gag-gLuc exosomes and GFP signals of Gag-GFP exosomes were protected from ProK treatment

To evaluate the resistance of gLuc activity to ProK treatment, gLuc activity of Gag-gLuc exosomes and gLuc-LA exosomes was measured after ProK treatment. gLuc activity of Gag-gLuc exosomes was not reduced by ProK treatment (99.3%), whereas gLuc activity of gLuc-LA exosome almost completely absent (0.05%) after the digestion (Fig. 10a). I additionally confirmed that Gag-based fusion proteins were resistant to ProK treatment by observing PKH26-labeled Gag-GFP exosomes and GFP-LA exosomes under a fluorescent microscope. Figure 10b shows that the GFP signals colocalized with the red signals of PKH26-labeled exosomes in the Gag-GFP exosomes. However, for GFP-LA exosomes, the GFP signal disappeared after ProK treatment, while the red signal of PKH26-labeled exosomes was retained. These results indicate that Gag-fusion proteins are not digested by ProK treatment, suggesting that Gag-fusion proteins are located inside of exosomes.

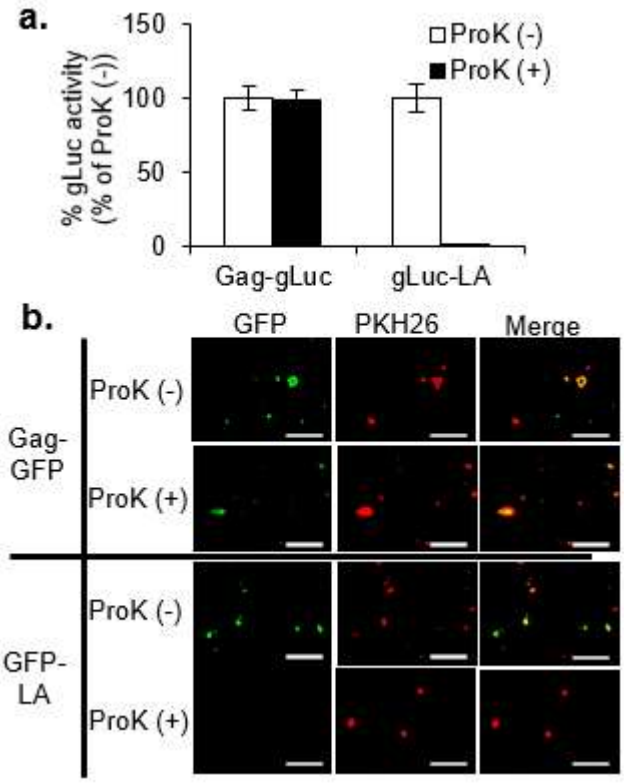

Figure 10. Gag-based fusion proteins on the interior of exosomes were resistant to proteinase K (ProK) digestion. (a) Gag-gLuc exosomes and gLuc-LA exosomes were digested by ProK, and then luciferase activity was measured. The data are expressed as the mean ± standard deviation (n = 3). (b) Gag-GFP exosomes and GFP-LA exosomes were treated with ProK and then observed by fluorescence microscopy. Scale bar = 20 μm.

2-3-4. ProK treatment digested surface proteins of exosomes without altering their physicochemical properties

To evaluate the digestion of exosomal proteins by ProK, untreated and ProK-treated exosome samples were subjected to SDS-PAGE followed by CBB staining. Figure 11a shows that some protein bands found in untreated exosomes disappeared in ProK-treated exosomes, indicating that ProK digested some exosome proteins under this condition. Figure 11b shows the western blotting analysis of exosome marker proteins in untreated and ProK-treated exosomes. Both samples were positive for Alix, an exosome marker protein localized to the interior of exosomes. I detected CD81, a tetraspanin exosome marker protein, using an antibody which reacts against helical and extracellular domains of CD81. CD81 was negative in ProK-treated exosome samples, which suggests degradation of exosome surface proteins by ProK treatment. Figure 11c shows TEM images of the untreated and ProK-treated exosomes. Globular vesicles approximately 100 nm in diameter were observed in both exosome samples. As shown in Figure 11d-f, untreated and ProK-treated exosomes showed

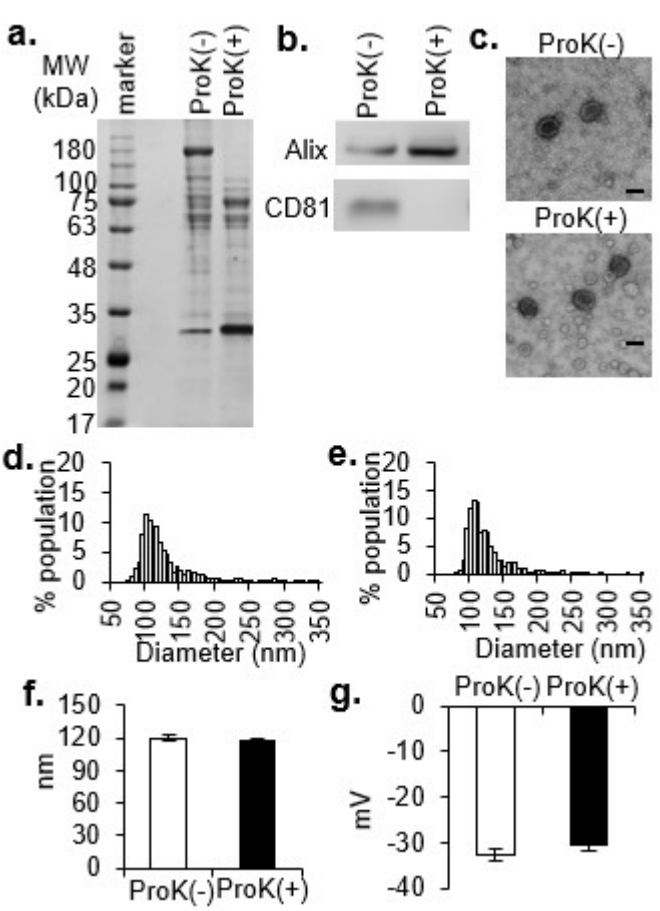

Figure 11. Effect of ProK treatment on exosome protein and physicochemical properties. (a) Coomassie Brilliant Blue (CBB) staining of untreated and ProK-treated normal exosomes. Lane 1: Marker. Lane 2: Untreated exosomes. Lane 3: ProK-treated exosomes. (b) Western blotting of Alix and CD81 in untreated (lane 1) and ProK treated normal exosomes (lane 2). (c) TEM images of untreated and ProK-treated normal exosomes. Scale bar = 100 μm. (d, e) Size distribution of untreated (d) and ProK-treated (e) normal exosomes. (f) Median size of untreated and ProK-treated normal exosomes calculated from qNano data. (g) Zeta potential of untreated and ProKtreated normal exosomes. The data are expressed as the mean ± standard deviation (n = 3).

similar size distribution and were 120 ± 3 nm and 117 ± 3 nm in diameter, respectively. Figure 11g shows that untreated and ProK-treated exosomes possessed comparable negative zeta potential, which were -32.7 ± 1.3 mV and -30.5 ± 1.3 mV, respectively. These results indicate that ProK can digest the surface proteins of exosome, but it minimally alters the physicochemical properties of exosomes.

2-3-5. ProK treatment of exosomes slightly increased their serum concentration after intravenous injection to mice

To evaluate the role of surface proteins of exosomes in pharmacokinetics, Gag-gLuc exosomes were digested with ProK, then the exosomes were intravenously injected into mice (Fig. 12). The level of initial serum concentration of Gag-gLuc exosomes treated with ProK was moderately, but significantly higher than that of the untreated group (Fig. 12a). Although the MRT and half-life did not change (Fig. 12c-d), the area under the curve (AUC) (Fig. 12b) of the ProK-treated group was significantly 1.7-fold higher than that of the untreated group.

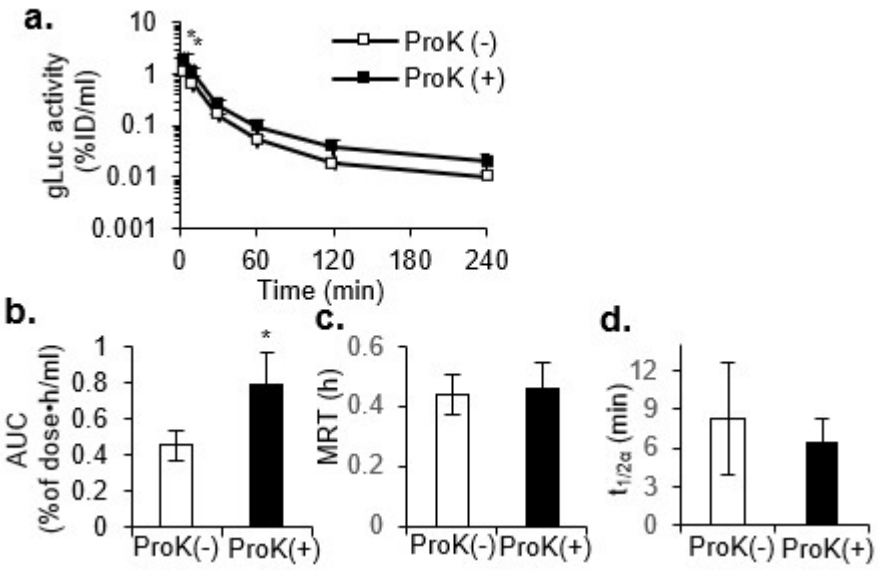

Figure 12. Time course of serum gLuc activity after intravenous injection of untreated and ProK-treated Gag-gLuc exosomes. (a) Serum gLuc activity was measured after intravenous injection of untreated and ProK-digested Gag-gLuc exosomes. These results are expressed as the mean ± standard deviation (n = 4). %ID: % of injected dose. Pharmacokinetic parameters of untreated and ProK-digested Gag-gLuc exosomes after intravenous injection, which are (b) AUC, (c) MRT, (d) t1/2, shown as histograms. *p < 0.05 compared to untreated group. AUC values of untreated and ProK-treated exosomes were 0.46 ± 0.08 and 0.79 ± 0.18% of dose·h/mL, respectively. MRT values of untreated and ProK-treated exosomes were 0.44 ± 0.07 and 0.46 ± 0.09 h, respectively. $t_{1/2}$ values of untreated and ProK-treated exosomes were 8.30 ± 4.32 and 6.42 ± 1.19 min, respectively.

2-3-6. ProK treatment did not affect uptake of exosomes by peritoneal macrophages

Since intravenously injected exosomes are mainly taken up by macrophages in the liver and spleen [11], I evaluated the effect of surface protein digestion by ProK on the uptake of exosomes by macrophages (Fig. 13). Mean fluorescent intensity of peritoneal macrophages incubated with untreated and ProK-treated exosomes labeled with PKH67 was determined by flow cytometry. Untreated and ProK-treated exosomes showed 28.1 ± 1.1 MFI and 27.7 ± 1.1 MFI at a concentration of 2.8 μg/ml and 120.5 ± 3.7 MFI and 121.0 ± 4.5 MFI at a concentration of 14 μg/ml, respectively. There was no significant difference in the fluorescent intensity of macrophages between untreated and ProK-treated exosome groups.

To evaluate the role of surface proteins in the uptake by macrophages in the liver, co-localizations of PKH26-labelled untreated and ProK-treated exosomes with macrophage in liver section were observed. It was shown that intravenously-administered exosomes were taken up by macrophage in the liver irrespective of ProK treatment (Fig. 13b). Quantification of red

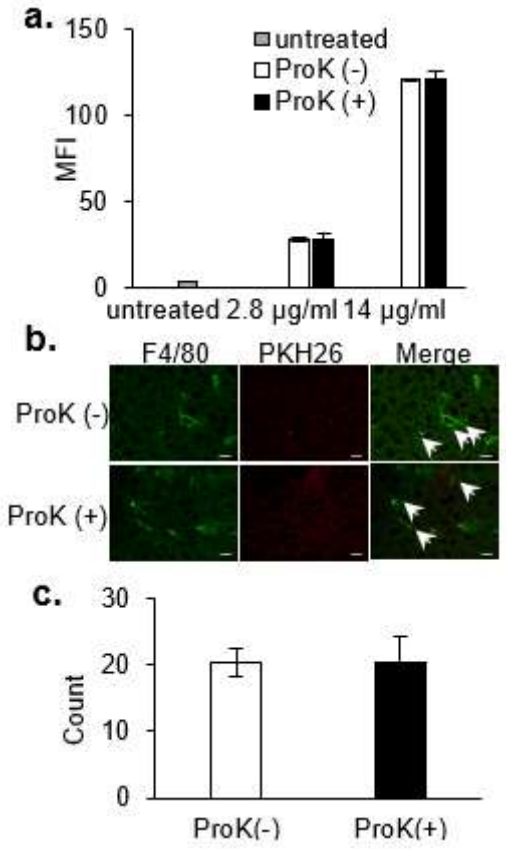

Figure 13. Uptake of untreated and ProK-treated exosomes by macrophages. (a) Peritoneal macrophages were incubated with untreated and ProK-treated PKH67-labeled exosomes, and then mean fluorescence intensity (MFI) was measured by flow cytometry. MFI values of untreated and ProK-treated exosomes were 28.1 ± 1.1 and 27.7 ± 1.1 at a concentration of 2.8 μg/mL and 120.5 ± 3.7 and 121.0 ± 4.5 at a concentration of 14 μg/mL, respectively. The data are expressed as the mean ± standard deviation (n = 4). (b) Cryostat sections of the liver collected from mice receiving PKH26-labeled exosomes (red) were stained with Alexa Fluor488-labeled anti-mouse F4/80 antibody (green). Arrowheads indicate colocalization of macrophage and exosomes. Scale bar = 10 μm. (c) Average number of red fluorescence signals was calculated from 20 fields/section. The data are expressed as the mean ± standard deviation (n = 3).

fluorescence signals showed that the amount of PKH26-labeled exosomes in the liver was comparable between untreated (20.3 ± 2.1 count) and ProK-treated (20.2 ± 4.2 count) groups. This result indicates that surface proteins are hardly involved in the uptake of exosomes by macrophages in the liver.

2-3-7. Degradation of surface proteins on exosome affected lung distribution of exosome

As it was demonstrated that $\alpha_6\beta_1$ integrin is related to lung distribution of melanoma-derived exosomes, I evaluated whether ProK treatment degraded integrin $\alpha_6\beta_1$ of exosomes. As shown in Fig. 7a, both integrin α_6 and integrin β_1 were degraded by ProK treatment. To evaluate the role of surface proteins in the distribution of exosomes to the lung, untreated and ProK-treated exosome labeled with PKH26 were injected into mice and lung sections were prepared and observed under fluorescence microscopy. Less red fluorescence was observed in the sections of lung collected from the ProK-treated exosome group (31.5 ± 4.0 counts) compared to the untreated exosome group (9.3 ± 1.0 counts) (Fig. 14a). Quantification of red fluorescence signals indicated that lung distribution of ProK-treated exosome was less than the untreated group (Fig. 14b). This result indicates that surface protein played a role in the lung distribution of exosomes.

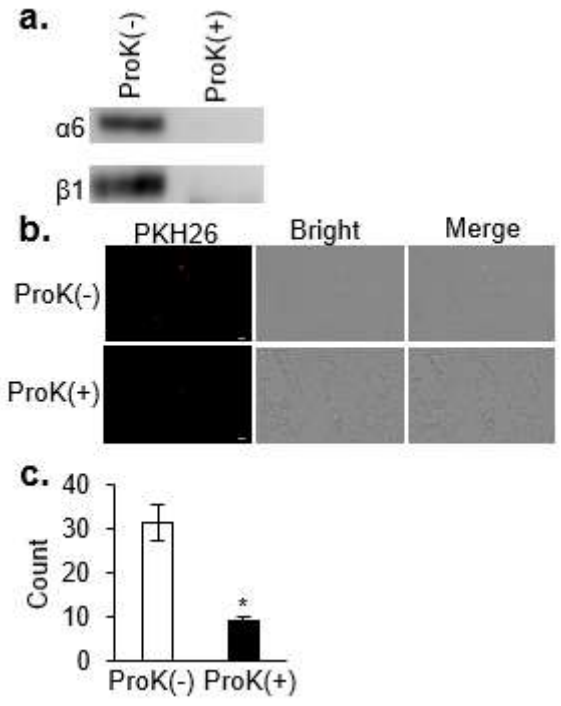

Figure 14. Lung distribution of untreated or ProK-treated PKH26-labeled exosomes. (a) Western blotting of integrin α_6 and integrin β_1 in untreated (left) and ProK-treated normal exosomes (right). (b, c) Mice were intravenously injected with exosomes. Then, 10 min after the injection, the lung samples were collected and prepared. (b) The lung samples were observed under fluorescence microscopy. (c) average number of red fluorescence signals was calculated from 20 fields/section. The data are expressed as the mean ± standard deviation from three mice. *p < 0.05 compared to untreated group.

2-4. Discussion

In the present study, I successfully labeled the inner space of exosomes by using Gag-based fusion proteins. Western blotting analysis of exosome marker proteins indicated that ProK could not digest proteins inside of the exosomes (Fig. 11). Therefore, ProK can be used for the evaluation of the role of surface proteins on exosomes. As Gag-based fusion proteins were resistant to ProK treatment, Gag-based fusion proteins appear to be located inside of exosomes (Fig. 10). Although CD63 has been widely used to label exosome membranes, Gag fusion proteins could modify exosome membranes more efficiently than CD63 because gLuc activity of Gag-gLuc exosomes was more than 100-fold higher than that of CD63-gLuc exosomes despite the fact that gLuc activity of cell lysates, which at least partly reflect the transgene expression level, was comparable between Gag-gLuc and CD63-gLuc groups. Therefore, Gag can be used to load cargoes into exosomes.

As proteinase treatment digests proteins located on the surface of exosomes, there was a possibility that properties of exosome, such as diameter and zeta potential, are affected by proteinase treatment [41]. I evaluated the total protein amount per particle of untreated and ProK-treated exosomes and found that approximately half of the total proteins in ProK-treated exosome were reduced (data not shown). Unexpectedly, although surface proteins were digested by ProK, ProK treatment had little effect on exosome physicochemical properties (Fig. 11). It was reported that the negative charge of cancer exosomes was due to the large amount of sialic acids, which are likely to be removed by ProK treatment [42]. On the other hand, as demonstrated in a previous report of my laboratory [31], phosphatidylserine, a negatively charged phospholipid, exists on the surface of exosome. As phosphatidylserine is not affected by ProK treatment, the negative zeta potential of ProK-treated exosome may be due to negatively charged lipids such as phosphatidylserine. As the physicochemical properties of delivery carrier such as size and zeta potential play important role in the pharmacokinetics of the carriers [43–45], the fact that ProK treatment minimally affected these characteristics of exosome suggests that ProK treatment can

be used for the evaluation of the roles of surface proteins on the pharmacokinetics of exosomes at the whole-body level in mice.

By using Gag-gLuc labeled exosome, I found that surface protein digestion of B16BL6-derived exosomes slightly, but significantly increased the AUC after intravenous injection of exosomes, but had little effect on other parameters. Since an increase in AUC by ProK treatment without altering the half-life implies a decrease in distribution volume, which may be explained by the decrease in the distribution to liver and lung, I evaluated the effect of ProK treatment on the distribution to these organs. Distribution to the liver mainly occurs through uptake of exosomes by macrophages, so I evaluated uptake of exosomes by macrophages and found that removal of exosome surface proteins did not affect the cellular uptake by macrophages. Moreover, an in vivo experiment clearly showed that distribution to the liver and the uptake by macrophages in the liver of exosomes after intravenous administration were hardly affected by ProK treatment. In contrast, integrin $\alpha_6\beta_1$ was degraded after ProK treatment. ProK-treated exosomes showed lower lung distribution than untreated exosomes, indicating that surface proteins of exosomes are important distribution of exosomes to the lungs. It has been demonstrated that integrin $\alpha_6\beta_1$ was expressed on melanoma cells [46] and increased exosome uptake in lung and promoted the adhesion of tumor exosome within lung [32]. Therefore, surface proteins of exosomes, such as integrin $\alpha_6\beta_1$, might be related to the lung distribution of B16BL6-derived exosomes. In previous study of my laboratory, it was demonstrated that the negative charge of PS in exosome membranes is involved in the exosome uptake by macrophages [31]. The result in the current study that surface protein digestion showed little effect on exosome uptake by macrophages supports the hypothesis that PS, not protein, is the major component recognized by macrophages.

In Chapter 2, I have developed inner membrane modification method using Gag fusion protein. Using Gag fusion proteins, I revealed that some surface proteins such as integrin $\alpha_6\beta_1$ play role in their pharmacokinetics at the whole body level in mice.

Chapter 3

Development of preservation method of exosomes at room temperature by using lyophilization.

3-1. Summary

The applications of exosomes can be expanded by the development of an appropriate preservation method. Exosomes are generally stored at -80 °C[47], this temperature is not suitable for their handling or transportation. Lyophilization is a promising storage method that can be used to preserve various substances at room temperature. Currently, no data is available to suggest whether lyophilization is applicable to exosomes or not.

In this chapter, I first developed a method to lyophilize exosomes derived from B16BL6 melanoma cells by using trehalose, as a cryoprotectant [48–50]. Next, I investigated the effect of lyophilization on the physical properties of exosomes. Finally, I evaluated the pharmacokinetics, exosomal protein and RNA content, and the activity of cargo proteins and DNA, in lyophilized exosomes and those stored at -80 °C.

It was found that lyophilization without cryoprotectant resulted in the aggregation of exosomes, while the addition of trehalose, a cryoprotectant, prevented aggregation during lyophilization. PAGE analysis revealed that the proteins and RNA of exosomes were protected following lyophilization in the presence of trehalose. Lyophilization had little effect on the pharmacokinetics of Gaussia luciferase (gLuc)-labeled exosomes after an intravenous injection into mice. Moreover, it was found that lyophilized exosomes retained the activity of loaded gLuc and immunostimulatory CpG DNA for more than a week even when stored at 25 °C, indicating that lyophilization may be utilized to preserve exosomes loaded with pharmacologically active functional molecules.

In this chapter, I have succeeded in the development of room temperature preservation method of exosome using lyophilization with trehalose. Exosomal proteins and RNAs were preserved in lyophilized exosomes. In addition, physicochemical and pharmacokinetic properties were retained in lyophilized exosomes. Furthermore, using lyophilization, biologically active molecules loaded into exosome could be preserved at room temperature. These findings may provide useful information about preservation method of exosome for using exosome as DDS.

Summary

Exosomes have potential to be used as drug delivery carriers. To exploit exosomes as drug delivery carriers, I have evaluated the pharmacokinetic and pharmaceutical characteristics of exosomes for the development of exosome-based drug delivery carrier over these 3 chapters.

Chapter 1: Evaluation of cell type-specific and common characteristics of exosomes derived from mouse cell lines

I demonstrated that the five different cell types produced different yields of exosomes. All of the exosomes produced were comparable physicochemical and pharmacokinetic properties after intravenous injection into mice. These results imply that it is desirable to select various types of exosome-producing cells from the viewpoint of productivity, such as exosome yield and ease of handling, when developing exosome-based DDS.

Chapter 2: Evaluation of the role of exosome surface proteins in the pharmacokinetics of exosome

I demonstrated that Gag protein can be used for labeling the inner surface of exosome and that untreated or ProK-treated exosomes showed comparable physicochemical properties and slightly different pharmacokinetics. Moreover, I found that surface proteins play some roles in pharmacokinetics of exosomes at the whole-body level in mice.

Chapter 3: Development of preservation method of exosomes at room temperature by using lyophilization.

I demonstrated that trehalose could be used to prevent exosomal damage during lyophilization. Moreover, it was found that the storage of lyophilized exosomes at room temperature did not affect protein and RNA content, physicochemical and pharmacokinetics

properties, or the function of protein and DNA loaded on exosomes. These findings may provide useful information about preservation method of exosome for using exosome as DDS.

In conclusion of my thesis, I demonstrated that types of cells poorly affected the physicochemical and pharmacokinetics of exosomes. I also found that surface proteins of exosomes play a role in the pharmacokinetics of exosomes. Moreover, I developed room temperature preservation method of exosomes using lyophilization in the presence of cryoprotectant. The findings of this thesis may provide useful information for the development of exosome-based drug delivery systems.

Acknowledgements

Firstly, I would like to express my sincere gratitude to my advisor Dr. Yoshinobu Takakura, Professor of Department of Biopharmaceutics and Drug Metabolism, Graduate School of Pharmaceutical Sciences, Kyoto University for giving me wonderful opportunities to join this wonderful laboratory, and his excellent guidance, valuable discussion, warm support and encouragement. His guidance helped me in all the time of research and writing of this thesis.

Also, I am extremely grateful to my research guides, Dr. Yuki Takahashi, Associate Professor of Department of Biopharmaceutics and Drug Metabolism. It was a great opportunity to do my doctoral program under his guidance and to learn from his research expertise. All of his encouragement, insightful comments, and hard questions are fully helpful and essential for my Ph.D. course. I could not have imagined having a better advisor and mentor for my Ph.D study.

I wish to express my deepest appreciation to Dr. Makiya Nishikawa, Professor of Laboratory of Biopharmaceutics, Faculty of Pharmaceutical Sciences, Tokyo University of Science for his patient supervision, insightful comments, suggestions, guidance and direction, valuable discussions and supports facilitating the successful completion of this study throughout the whole this study.

I would like to thank all labmates, both the alumni and present members of Department of Biopharmaceutics and Drug metabolism and of Drug Delivery Research, Graduate School of Pharmaceutics Sciences, Kyoto University for the stimulating discussions for their experimental assistances, and for all the fun we have had in these five years.

This thesis would have not been possible without the scholarship and financial support for my higher graduate studies from Ministry of Education, Culture, Sports, Science and Technology of Japanese Government.

Then, I would like to thank to my Thai friends in Kyoto, for their warm friendship, for all of support in my hard times of study abroad life, and for spending valuable time together in Kyoto.

Last but not the least, I would like to thank my family: my parents and to my sister, for their infinite love, encouragement, and spiritual support that helped me to get through tough times during my PhD course and my life in general.

List of Publications

Cell type-specific and common characteristics of exosomes derived from mouse cell lines: Yield, physicochemical properties, and pharmacokinetics.

Chonlada Charoenviriyakul, Yuki Takahashi, Masaki Morishita, Akihiro Matsumoto, Makiya Nishikawa, Yoshinobu Takakura.

European Journal of Pharmaceutical Sciences 2017, 96, 316–322

Role of Extracellular Vesicle Surface Proteins in the Pharmacokinetics of Extracellular Vesicles

Chonlada Charoenviriyakul, Yuki Takahashi, Masaki Morishita, Makiya Nishikawa, Yoshinobu Takakura.

Molecular Pharmaceutics 2018, 15, 1073−1080

Preservation method of exosomes at room temperature by using lyophilization.

Chonlada Charoenviriyakul, Yuki Takahashi, Makiya Nishikawa, Yoshinobu Takakura.

Manuscript submitted

List of Other Publications

Macrophage-dependent clearance of systemically administered B16BL6-derived exosomes from the blood circulation in mice

Takafumi Imai, Yuki Takahashi, Makiya Nishikawa, Kana Kato, Masaki Morishita, Takuma Yamashita, Akihiro Matsumoto, Chonlada Charoenviriyakul, Yoshinobu Takakura

Journal of Extracellular Vesicles 2015, 4, 26238

Role of Phosphatidylserine-Derived Negative Surface Charges in the Recognition and Uptake of Intravenously Injected B16BL6-Derived Exosomes by Macrophages

Akihiro Matsumoto, Yuki Takahashi, Makiya Nishikawa, Kohei Sano, Masaki Morishita, Chonlada Charoenviriyakul, Hideo Saji, Yoshinobu Takakura

Journal of Pharmaceutical Sciences 2017, 106, 168-175

Accelerated growth of B16BL6 tumor in mice through efficient uptake of their own exosomes by B16BL6 cells

Akihiro Matsumoto, Yuki Takahashi, Makiya Nishikawa, Kohei Sano, Masaki Morishita,Chonlada Charoenviriyakul, Hideo Saji, Yoshinobu Takakura

Cancer Sciences 2017, 108, 1803–1810

References

(1) EL Andaloussi, S.; Mäger, I.; Breakefield, X. O.; Wood, M. J. A. Extracellular Vesicles: Biology and Emerging Therapeutic Opportunities. *Nat. Rev. Drug Discov.* **2013**, *12* (5), 347–357.

(2) Ha, D.; Yang, N.; Nadithe, V. Exosomes as Therapeutic Drug Carriers and Delivery Vehicles across Biological Membranes: Current Perspectives and Future Challenges. *Acta Pharm. Sin. B* **2016**, *6* (4), 287–296.

(3) Johnsen, K. B.; Gudbergsson, J. M.; Skov, M. N.; Pilgaard, L.; Moos, T.; Duroux, M. A Comprehensive Overview of Exosomes as Drug Delivery Vehicles — Endogenous Nanocarriers for Targeted Cancer Therapy. *Biochim. Biophys. Acta - Rev. Cancer* **2014**, *1846* (1), 75–87.

(4) Vlassov, A. V.; Magdaleno, S.; Setterquist, R.; Conrad, R. Exosomes: Current Knowledge of Their Composition, Biological Functions, and Diagnostic and Therapeutic Potentials. *Biochim. Biophys. Acta - Gen. Subj.* **2012**, *1820* (7), 940–948.

(5) Bobrie, A.; Colombo, M.; Raposo, G.; Théry, C. Exosome Secretion: Molecular Mechanisms and Roles in Immune Responses. *Traffic* **2011**, *12* (12), 1659–1668.

(6) Iero, M.; Valenti, R.; Huber, V.; Filipazzi, P.; Parmiani, G.; Fais, S.; Rivoltini, L. Tumour-Released Exosomes and Their Implications in Cancer Immunity. *Cell Death Differ.* **2008**, *15* (1), 80–88.

(7) Théry, C.; Ostrowski, M.; Segura, E. Membrane Vesicles as Conveyors of Immune Responses. *Nat. Rev. Immunol.* **2009**, *9* (8), 581–593.

(8) Alvarez-Erviti, L.; Seow, Y.; Yin, H.; Betts, C.; Lakhal, S.; Wood, M. J. A. Delivery of siRNA to the Mouse Brain by Systemic Injection of Targeted Exosomes. *Nat. Biotechnol.* **2011**, *29* (4), 341–345.

(9) Tian, Y.; Li, S.; Song, J.; Ji, T.; Zhu, M.; Anderson, G. J.; Wei, J.; Nie, G. A Doxorubicin Delivery Platform Using Engineered Natural Membrane Vesicle Exosomes for Targeted Tumor Therapy. *Biomaterials* **2014**, *35* (7), 2383–2390.

(10) Takahashi, Y.; Nishikawa, M.; Shinotsuka, H.; Matsui, Y.; Ohara, S.; Imai, T.; Takakura, Y. Visualization and in Vivo Tracking of the Exosomes of Murine Melanoma B16-BL6 Cells in Mice after Intravenous Injection. *J. Biotechnol.* **2013**, *165* (2), 77–84.

(11) Imai, T.; Takahashi, Y.; Nishikawa, M.; Kato, K.; Morishita, M.; Yamashita, T.; Matsumoto, A.; Charoenviriyakul, C.; Takakura, Y. Macrophage-Dependent Clearance of Systemically Administered B16BL6-Derived Exosomes from the Blood Circulation in Mice. *J. Extracell. vesicles* **2015**, *4*, 26238.

(12) Yamashita, T.; Takahashi, Y.; Nishikawa, M.; Takakura, Y. Effect of Exosome Isolation Methods on Physicochemical Properties of Exosomes and Clearance of Exosomes from the Blood Circulation. *Eur. J. Pharm. Biopharm.* **2016**, *98*, 1–8.

(13) Yeo, R. W. Y.; Lai, R. C.; Zhang, B.; Tan, S. S.; Yin, Y.; Teh, B. J.; Lim, S. K. Mesenchymal Stem Cell: An Efficient Mass Producer of Exosomes for Drug Delivery. *Adv. Drug Deliv. Rev.* **2013**, *65* (3), 336–341.

(14) Ohno, S.; Takanashi, M.; Sudo, K.; Ueda, S.; Ishikawa, A.; Matsuyama, N.; Fujita, K.; Mizutani, T.; Ohgi, T.; Ochiya, T.; et al. Systemically Injected Exosomes Targeted to EGFR Deliver Antitumor MicroRNA to Breast Cancer Cells. *Mol. Ther.* **2013**, *21* (1), 185–191.

(15) Zhuang, X.; Xiang, X.; Grizzle, W.; Sun, D.; Zhang, S.; Axtell, R. C.; Ju, S.; Mu, J.; Zhang, L.; Steinman, L.; et al. Treatment of Brain Inflammatory Diseases by Delivering Exosome Encapsulated Anti-Inflammatory Drugs from the Nasal Region to the Brain. *Mol. Ther.* **2011**, *19* (10), 1769–1779.

(16) Katakowski, M.; Buller, B.; Zheng, X.; Lu, Y.; Rogers, T.; Osobamiro, O.; Shu, W.; Jiang, F.; Chopp, M. Exosomes from Marrow Stromal Cells Expressing miR-146b Inhibit Glioma Growth. *Cancer Lett.* **2013**, *335* (1), 201–204.

(17) Rana, S.; Yue, S.; Stadel, D.; Zöller, M. Toward Tailored Exosomes: The Exosomal Tetraspanin Web Contributes to Target Cell Selection. *Int. J. Biochem. Cell Biol.* **2012**, *44* (9), 1574–1584.

(18) Ban, J.-J.; Lee, M.; Im, W.; Kim, M. Low pH Increases the Yield of Exosome Isolation. *Biochem. Biophys. Res. Commun.* **2015**, *461* (1), 76–79.

(19) Fauré, J.; Lachenal, G.; Court, M.; Hirrlinger, J.; Chatellard-Causse, C.; Blot, B.; Grange, J.; Schoehn, G.; Goldberg, Y.; Boyer, V.; et al. Exosomes Are Released by Cultured Cortical Neurones. *Mol. Cell. Neurosci.* **2006**, *31* (4), 642–648.

(20) Ji, H.; Erfani, N.; Tauro, B. J.; Kapp, E. A.; Zhu, H.; Moritz, R. L.; Lim, J. W. E.; Simpson, R. J. Difference Gel Electrophoresis Analysis of Ras-transformed Fibroblast Cell-derived Exosomes. *Electrophoresis* **2008**, *29* (12), 2660–2671.

(21) Singh, P. P.; Smith, V. L.; Karakousis, P. C.; Schorey, J. S. Exosomes Isolated from Mycobacteria-Infected Mice or Cultured Macrophages Can Recruit and Activate Immune Cells In Vitro and In Vivo. *J. Immunol.* **2012**, *189* (2), 777–785.

(22) Sokolova, V.; Ludwig, A.-K.; Hornung, S.; Rotan, O.; Horn, P. A.; Epple, M.; Giebel, B. Characterisation of Exosomes Derived from Human Cells by Nanoparticle Tracking

Analysis and Scanning Electron Microscopy. *Colloids Surfaces B Biointerfaces* **2011**, *87* (1), 146–150.

(23) Madison, R. D.; McGee, C.; Rawson, R.; Robinson, G. A. Extracellular Vesicles from a Muscle Cell Line (C2C12) Enhance Cell Survival and Neurite Outgrowth of a Motor Neuron Cell Line (NSC-34). *J. Extracell. Vesicles* **2014**, *3* (1), 22865.

(24) Nazarenko, I.; Rana, S.; Baumann, A.; McAlear, J.; Hellwig, A.; Trendelenburg, M.; Lochnit, G.; Preissner, K. T.; Zöller, M. Cell Surface Tetraspanin Tspan8 Contributes to Molecular Pathways of Exosome-Induced Endothelial Cell Activation. *Cancer Res.* **2010**, *70* (4), 1668–1678.

(25) Hazawa, M.; Tomiyama, K.; Saotome-Nakamura, A.; Obara, C.; Yasuda, T.; Gotoh, T.; Tanaka, I.; Yakumaru, H.; Ishihara, H.; Tajima, K. Radiation Increases the Cellular Uptake of Exosomes through CD29/CD81 Complex Formation. *Biochem. Biophys. Res. Commun.* **2014**, *446* (4), 1165–1171.

(26) Smyth, T.; Kullberg, M.; Malik, N.; Smith-Jones, P.; Graner, M. W.; Anchordoquy, T. J. Biodistribution and Delivery Efficiency of Unmodified Tumor-Derived Exosomes. *J. Control. Release* **2015**, *199*, 145–155.

(27) Wiklander, O. P. B.; Nordin, J. Z.; O'Loughlin, A.; Gustafsson, Y.; Corso, G.; Mäger, I.; Vader, P.; Lee, Y.; Sork, H.; Seow, Y.; et al. Extracellular Vesicle in Vivo Biodistribution Is Determined by Cell Source, Route of Administration and Targeting. *J. Extracell. vesicles* **2015**, *4*, 26316.

(28) Fadok, V. A.; Voelker, D. R.; Campbell, P. A.; Cohen, J. J.; Bratton, D. L.; Henson, P. M. Exposure of Phosphatidylserine on the Surface of Apoptotic Lymphocytes Triggers Specific Recognition and Removal by Macrophages. *J. Immunol.* **1992**, *148* (7), 2207–2216.

(29) Théry, C.; Zitvogel, L.; Amigorena, S. Exosomes: Composition, Biogenesis and Function. *Nat. Rev. Immunol.* **2002**, *2* (8), 569–579.

(30) Watson, D. C.; Bayik, D.; Srivatsan, A.; Bergamaschi, C.; Valentin, A.; Niu, G.; Bear, J.; Monninger, M.; Sun, M.; Morales-Kastresana, A.; et al. Efficient Production and Enhanced Tumor Delivery of Engineered Extracellular Vesicles. *Biomaterials* **2016**, *105*, 195–205.

(31) Matsumoto, A.; Takahashi, Y.; Nishikawa, M.; Sano, K.; Morishita, M.; Charoenviriyakul, C.; Saji, H.; Takakura, Y. Role of Phosphatidylserine-Derived Negative Surface Charges in the Recognition and Uptake of Intravenously Injected B16BL6-Derived Exosomes by Macrophages. *J. Pharm. Sci.* **2017**, *106* (1), 168–175.

(32) Hoshino, A.; Costa-Silva, B.; Shen, T.-L.; Rodrigues, G.; Hashimoto, A.; Tesic Mark, M.; Molina, H.; Kohsaka, S.; Di Giannatale, A.; Ceder, S.; et al. Tumour Exosome Integrins Determine Organotropic Metastasis. *Nature* **2015**, *527* (7578), 329–335.

(33) Suomalainen, M.; Hultenby, K.; Garoff, H. Targeting of Moloney Murine Leukemia Virus Gag Precursor to the Site of Virus Budding. *J. Cell Biol.* **1996**, *135* (6 Pt 2), 1841–1852.

(34) Hamard-Peron, E.; Juillard, F.; Saad, J. S.; Roy, C.; Roingeard, P.; Summers, M. F.; Darlix, J.-L.; Picart, C.; Muriaux, D. Targeting of Murine Leukemia Virus Gag to the Plasma Membrane Is Mediated by PI(4,5)P2/PS and a Polybasic Region in the Matrix. *J. Virol.* **2010**, *84* (1), 503–515.

(35) Takiguchi, N.; Takahashi, Y.; Nishikawa, M.; Matsui, Y.; Fukuhara, Y.; Oushiki, D.; Kiyose, K.; Hanaoka, K.; Nagano, T.; Takakura, Y. Positive Correlation Between the Generation of Reactive Oxygen Species and Activation/Reactivation of Transgene Expression After Hydrodynamic Injections into Mice. *Pharm. Res.* **2011**, *28* (4), 702–711.

(36) Heusermann, W.; Hean, J.; Trojer, D.; Steib, E.; von Bueren, S.; Graff-Meyer, A.; Genoud, C.; Martin, K.; Pizzato, N.; Voshol, J.; et al. Exosomes Surf on Filopodia to Enter Cells at Endocytic Hot Spots, Traffic within Endosomes, and Are Targeted to the ER. *J. Cell Biol.* **2016**, *213* (2), 173–184.

(37) Stickney, Z.; Losacco, J.; McDevitt, S.; Zhang, Z.; Lu, B. Development of Exosome Surface Display Technology in Living Human Cells. *Biochem. Biophys. Res. Commun.* **2016**, *472* (1), 53–59.

(38) Singh, R.; Pochampally, R.; Watabe, K.; Lu, Z.; Mo, Y.-Y. Exosome-Mediated Transfer of miR-10b Promotes Cell Invasion in Breast Cancer. *Mol. Cancer* **2014**, *13* (1), 256.

(39) Svensson, K. J.; Christianson, H. C.; Wittrup, A.; Bourseau-Guilmain, E.; Lindqvist, E.; Svensson, L. M.; Mörgelin, M.; Belting, M. Exosome Uptake Depends on ERK1/2-Heat Shock Protein 27 Signaling and Lipid Raft-Mediated Endocytosis Negatively Regulated by Caveolin-1. *J. Biol. Chem.* **2013**, *288* (24), 17713–17724.

(40) Matsumoto, Y.; Kano, M.; Akutsu, Y.; Hanari, N.; Hoshino, I.; Murakami, K.; Usui, A.; Suito, H.; Takahashi, M.; Otsuka, R.; et al. Quantification of Plasma Exosome Is a Potential Prognostic Marker for Esophageal Squamous Cell Carcinoma. *Oncol. Rep.* **2016**, *36* (5), 2535–2543.

(41) Fernandes, H. P.; Cesar, C. L.; Barjas-Castro, M. de L. Electrical Properties of the Red Blood Cell Membrane and Immunohematological Investigation. *Rev. Bras. Hematol. Hemoter.* **2011**, *33* (4), 297–301.

(42) Akagi, T.; Kato, K.; Hanamura, N.; Kobayashi, M.; Ichiki, T. Evaluation of Desialylation Effect on Zeta Potential of Extracellular Vesicles Secreted from Human Prostate Cancer Cells by on-Chip Microcapillary Electrophoresis. *Jpn. J. Appl. Phys.* **2014**, *53* (6S), 06JL01.

(43) Albanese, A.; Tang, P. S.; Chan, W. C. W. The Effect of Nanoparticle Size, Shape, and Surface Chemistry on Biological Systems. *Annu. Rev. Biomed. Eng.* **2012**, *14* (1), 1–16.

(44) Fröhlich, E. The Role of Surface Charge in Cellular Uptake and Cytotoxicity of Medical Nanoparticles. *Int. J. Nanomedicine* **2012**, *7*, 5577.

(45) Li, S.-D.; Huang, L. Pharmacokinetics and Biodistribution of Nanoparticles. *Mol. Pharm.* **2008**, *5* (4), 496–504.

(46) Kuphal, S.; Bauer, R.; Bosserhoff, A.-K. Integrin Signaling in Malignant Melanoma. *Cancer Metastasis Rev.* **2005**, *24* (2), 195–222.

(47) Jeyaram, A.; Jay, S. M. Preservation and Storage Stability of Extracellular Vesicles for Therapeutic Applications. *AAPS J.* **2018**, *20* (1), 1.

(48) Kundu, A. K.; Chandra, P. K.; Hazari, S.; Ledet, G.; Pramar, Y. V.; Dash, S.; Mandal, T. K. Stability of Lyophilized siRNA Nanosome Formulations. *Int. J. Pharm.* **2012**, *423* (2), 525–534.

(49) Stark, B.; Pabst, G.; Prassl, R. Long-Term Stability of Sterically Stabilized Liposomes by Freezing and Freeze-Drying: Effects of Cryoprotectants on Structure. *Eur. J. Pharm. Sci.* **2010**, *41* (3–4), 546–555.

(50) Guan, T.; Miao, Y.; Xu, L.; Yang, S.; Wang, J.; He, H.; Tang, X.; Cai, C.; Xu, H. Injectable Nimodipine-Loaded Nanoliposomes: Preparation, Lyophilization and Characteristics. *Int. J. Pharm.* **2011**, *410* (1–2), 180–187.